

Study of the Beltline Weld and Base Metal of WWER-440 First Generation Reactor Pressure Vessel

J. Schuhknecht, U. Rindelhardt, and H.-W. Viehrig

Forschungszentrum Dresden-Rossendorf (FZD), Dresden, Germany

УДК 539.4

Исследование материалов бандажного сварного шва и основного металла реактора первого поколения ВВЭР-440

Я. Шукнехт, У. Риндельхардт, Г.-В. Фиериг

Исследовательский центр Дрезден-Россендорф, Дрезден, Германия

Представлены результаты исследования материалов бандажного сварного шва и кольца основного металла сосуда давления первого блока реактора типа ВВЭР-440/230. Исследовали круглые вырезки материала (трепаны) после радиационного облучения с последующим отжигом и повторным облучением. Основная задача рабочей программы исследований состояла в получении распределения механических характеристик реакторных сталей по толщине стенки реактора. Согласно стандарту ASTM E192 определялась базисная температура T_0 с целью оценки распределения вязкости разрушения по толщине стенки реактора.

Ключевые слова: реакторы типа ВВЭР, реакторные стали, металл сварного шва, основной металл, трепан, сварной шов, вязкость разрушения, метод Master Curve, образец типа Шарпи с V-образным надрезом.

Introduction. Nuclear plant operators must guarantee that the structural integrity of nuclear reactor pressure vessels (RPV) is assured during routine operations or under postulated accident conditions. The ageing of the RPV steels is monitored with surveillance program results or predicted by trend curves. However, embrittlement forecast via trend curves and surveillance specimens may not reflect the reality. Accordingly, the most realistic evaluation of the fracture toughness response of RPV material to irradiation is performed directly on RPV wall samples from decommissioned NPPs. Such a unique opportunity is now offered with material from the decommissioned Greifswald NPP (WWER-440/230). The four Greifswald NPP units representing the first generation of WWER-440 reactors were shutdown in 1990 after 11–17 years of operation [1]. Table 1 presents the operation characteristics of the Units 1 to 4 and the expected neutron fluences. RPVs in three different conditions are available:

- (i) Unit 1 is irradiated, annealed, and reirradiated (IAI);
- (ii) Units 2 and 3 are irradiated and annealed (IA);
- (iii) Unit 4 is irradiated.

The well-documented different irradiation/annealing states of the four decommissioned Greifswald RPVs [2] ensure validation of the material properties under long-term low flux irradiation during industrial recovery annealing and

T a b l e 1

Operation Characteristics and Expected Maximum Neutron Fluences of Greifswald Units 1 to 4

Unit	Operation period		Effective days	Annealed in	Azimuthal maximum of $N_{E>0.5\text{MeV}}$ in units of 10^{19} n/cm^2			
	date	cycles			inner wall axial maximum	inner wall weld 4	outer wall axial maximum	outer wall weld 4
1	1974–1988	13	4205.0	1988	5.53	3.93	1.40	0.96
1*	1988–1990	2	627.4	–	0.16	0.10	0.05	0.03
2	1975–1990	14	4067.4	1990	6.68	4.70	1.70	1.16
3	1978–1990	12	3581.8	1990	4.40	3.40	0.68	0.50
4	1979–1990	11	3207.9	not	4.00	3.10	0.62	0.45

* Reirradiated.

during subsequent reirradiation. Trepanns were extracted from the Units 1, 2, and 4. We present results of the circumferential core weld SN0.1.4 and the base metal ring 0.3.1 of the RPV from the Unit 1 of the Greifswald WWER-440/230.

Material and Specimens. The critical temperature of brittleness from the circumferential beltline welding seam SN0.1.4 of Greifswald Unit 1 RPV was estimated for the initial condition, T_{K0} , at 46°C, and after 13 campaigns of operation at 186°C (TK) [2]. In this state, the RPV was subjected to heat treatment at 475°C for 152 hours, in order to anneal the irradiation embrittlement in 1988. The RPV was heat-treated within a region of 0.7 m above and below the circumferential beltline welding seam No. SN0.1.4. After the annealing, compact specimens were taken from the weld metal at the inner vessel wall. Sub-size Charpy specimens were machined and tested. For these specimens the critical temperature of brittleness, TK, of 30°C was estimated [2]. After the annealing the operation of Unit 1 was continued for two more years (Table 1). Unit 1 was shutdown in 1990. Trepanns were extracted from the decommissioned Unit 1 RPV in 2005. The custom-built trepanning device and the trepanning procedure are described elsewhere [3].

Figure 1 shows the location of the trepanns taken from the RPV of Greifswald Unit 1, from the circumferential beltline welding seam SN0.1.4 and the base metal ring 0.3.1. At first, the trepanns from Unit 1 representing the IAI condition of the beltline welding seam were investigated. The WWER-440 RPV welding seams are X-butt multilayer submerged welds. They consist of a welding root welded with an unalloyed wire Sv-08A and the filling material welded with the alloyed wire Sv-10KhMFT. The chemical compositions measured at 3 locations of the welding seam belong to the alloyed filling material and generally agree with the information in the manufacturing protocol [2]. Cu and P contents are within the range specified in the manufacturing guidelines of the WWER-440/230, but both are clearly higher than in the specification of the next generation (model 213) with maximum allowed P and Cu contents of 0.01 and 0.1%, respectively [5].

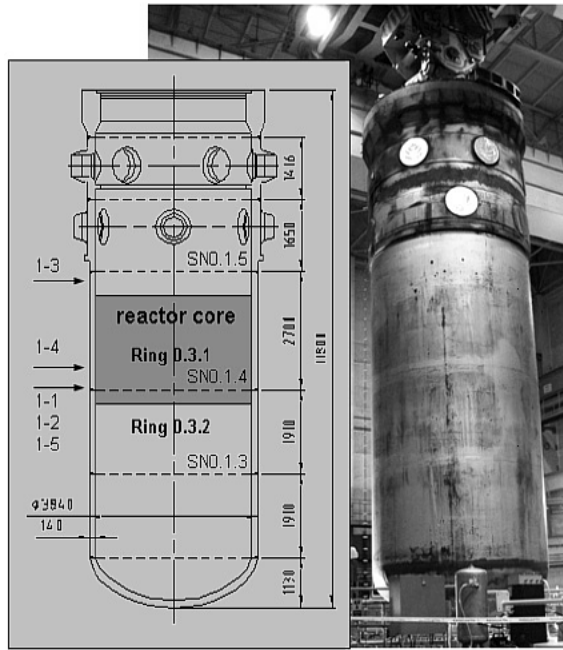


Fig. 1. RPV WWER 440 Greifswald Unit 1 and locations of the sampled trepans.

Trepans 1-1 and 1-4 were cut into discs each of 10 mm thickness using a wire travelling electro-erosion discharging machine (EDM). The location of the welding seam within trepan 1-1 was metallographically examined and depicted in Fig. 2 together with the cutting scheme of the disc 1-1.1. The welding root is located within a distance of about 60 to 80 mm relative to the inner RPV wall. The Charpy size SE(B) specimens were precracked ($a/W = 0.5$) and 20% side-grooved. As shown in Fig. 3, the orientation of the SE(B) specimen of the weld metal is TS (specimen axis and crack growth direction across the vessel wall) and for the base metal/trepan 1-4) is LS according to ASTM E399 [6]. The crack orientation is in correspondence with the surveillance specimens in Russian WWER-440/213 reactors.

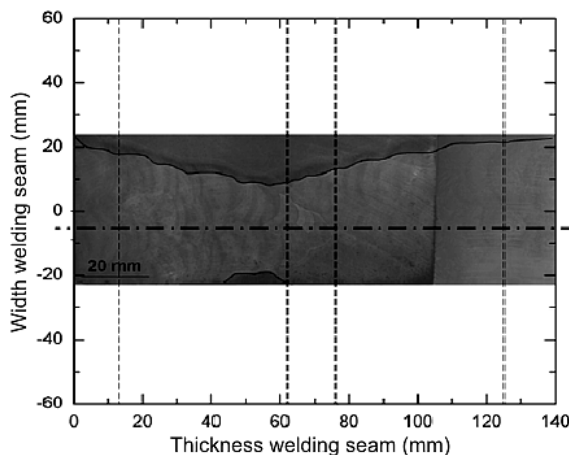


Fig. 2. Metallographic section of the welding seam trepan 1-1.

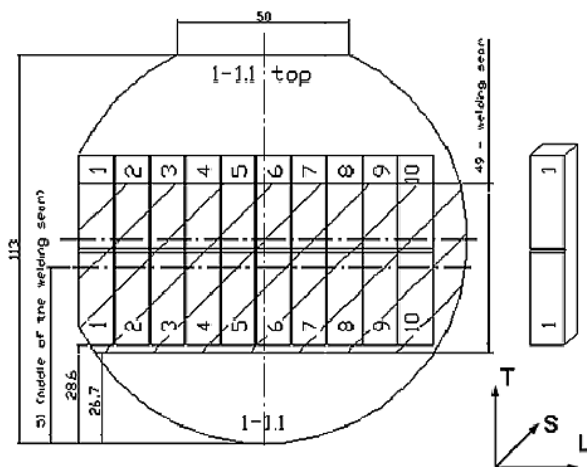


Fig. 3. Cutting scheme of disc 1-1.1.

Testing and Evaluation. SE(B) specimens representing 11 thickness locations of trepan 1-1 and 5 thickness locations from base metal trepan 1-4 were tested and evaluated according to ASTM E1921-05/08 [7]. The precracked and side-grooved Charpy size SE(B) specimens were monotonously loaded until they failed by cleavage instability. Standard Master Curve (MC) reference temperatures T_0 were evaluated with the measured J -integral-based cleavage fracture toughness values, K_{Jc} , applying the multitemperature procedure of ASTM E1921-05/08 [7]. In addition, the modified MC analysis of the SINTAP-procedure [8] was used for the evaluation of the measured K_{Jc} -values. The SINTAP lower tail analysis contains three steps, and guides the user towards the most appropriate estimate of the reference temperature, T_0^{SINTAP} , describing the samples having the lower toughness.

Instrumented Charpy V-notch impact tests on reconstituted specimens were performed according to DIN EN 10045-1 and EN ISO 14556. The impact energy, lateral expansion and fracture appearance temperature curves were fitted by the tanh approach. Such Charpy-V parameters as transition temperatures and the upper shelf energy were evaluated on specimens from different thickness locations.

Samples for metallographic investigations and hardness tests were prepared from selected tested specimens, in order to assess the structure in the vicinity of the fatigue crack tip.

Results and Discussion. Figure 4 illustrates the reference temperature T_0 evaluated according to ASTM E1921-05/08 and the Charpy-V transition temperature of the investigated discs of trepan 1-1. The background shows the design of the welding seam. Through the wall thickness, T_0 shows a wavelike behavior. After an initial increase of T_0 from 10°C at the inner surface to 50°C at 22 mm distance from it, T_0 decreases to 41°C at a distance of 70 mm, finally increasing to the maximum 67°C towards the outer RPV wall. The lowest T_0 value was measured in the root region of the welding seam representing a uniform fine-grain ferritic structure. Beyond the welding root T_0 shows a wavelike behavior with a span of about 50 K. Additionally, the MC SINTAP procedure was applied to determine

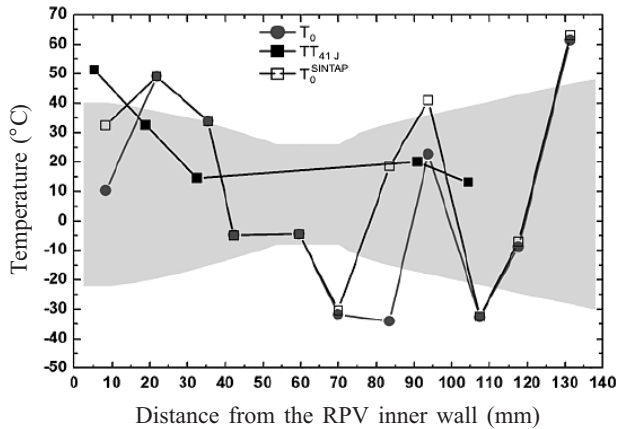


Fig. 4. Course of the reference temperatures T_0 through the welding seam SN0.1.4 of Greifswald Unit 1.

T_0^{SINTAP} representing the brittle fraction of the data set. For some thickness locations there are remarkable differences between T_0 and T_0^{SINTAP} values.

This strongly indicates that the material is not fully homogeneous, which is not unusual for the investigated multilayer weld metal. Figure 5 shows the K_{Jc} values versus the test temperature normalized to T_0 of the individual thickness location. The K_{Jc} values generally follow the course of the MC, though the scatter is large. Nevertheless, only 2 out of about 100 values of K_{Jc} lie below the 2% fracture probability line. As mentioned above, the beltline welding seam of Greifswald Unit 1 was recovery-annealed and reirradiated to low fluences.

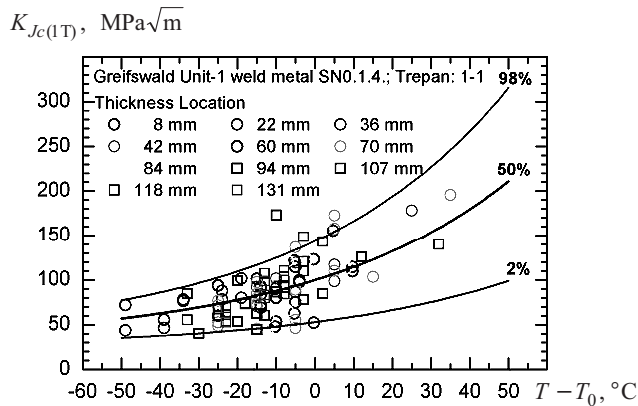


Fig. 5. K_{Jc} values of trepan 1-1 versus test temperature normalized to T_0 of the individual thickness location.

Taking into account that after 13 campaigns' operation $T_K = 186^\circ\text{C}$, the results presented here and those determined on subsize impact specimens [2] show that the embrittlement was almost fully undone due to the recovery-annealing. The re-embrittlement during 2 campaigns' operation can be assumed to be low. Hence, variation of T_0 measured through the thickness of the multilayer welding seam SN0.1.4 results basically from differences in the structure of the welding beads.

Figures 6 and 7 depict the structure in the vicinity of the crack tip of TS-oriented SE(B) specimens in different thickness locations. Generally, TS-oriented specimens have a uniform structure along the fatigue crack front (plane LS), thus crack tip is located in a varying uniform of the welding beads. Figure 6 shows the specimen structure from the thickness location 22 mm. The crack tip is located in a coarse-grain bainitic structure whose grains are framed with proeutectoid ferrite. This coarse-grain structure yields a T_0 of 49.1°C. For comparison, Fig. 7 shows the structure in the region of the welding root in a thickness location of 70 mm, where $T_0 = 40.6^\circ\text{C}$ was determined. There, the crack tip is located directly in a fine-grain structure of high ferrite content which was welded with the unalloyed wire Sv-08A.

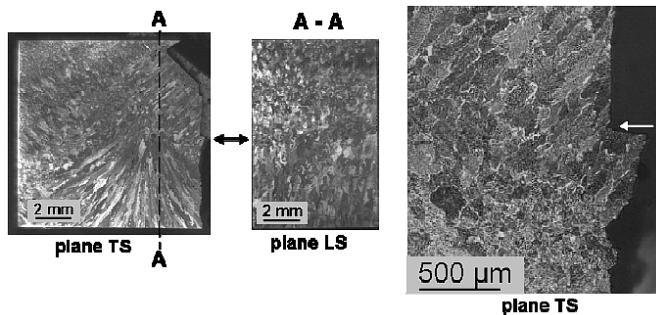


Fig. 6. Metallography of the filling (layer 22 mm).

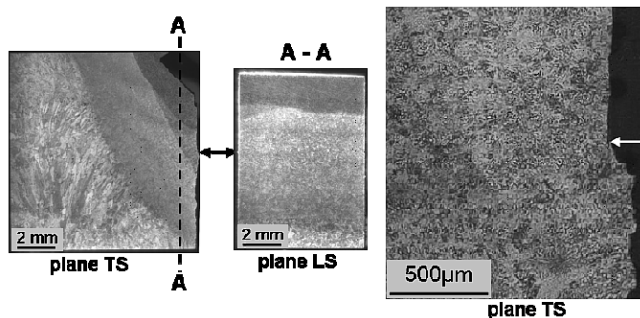


Fig. 7. Metallography of the root (70 mm).

This example demonstrates the effect of the specimen orientation on a multilayer welding seam. Unlike TS specimens, the structure of TL specimens varies along the fatigue crack front (plane LS), which is featured in the welding root region depicted in Fig. 7. It means that TS and TL specimens have a differentiating and integrating behavior, respectively. Therefore TS specimens are more sensitive to variations in the structure of the multilayer weld metal. The wide range of T_0 values spanning about 50 K can be explained by the location of the crack tip in the different structures of the welding beads.

According to the Russian regulatory guide PNAÉ-G-7-002-086 [9] the surveillance specimens of weld metal of WWER-440 (213) RPV origin from thickness locations beyond the welding root. The K_{Jc} values of the Sv-10KhMFT filling layers (distance of 84–118 mm from the inner surface) are evaluated separately. According to ASTM E1921-05 [7], T_0 of the overall evaluation is

20.9°C (Fig. 8) and the T_0^{SINTAP} evaluated with SINTAP of the more conservative step 3 is 22.3°C. As shown in Fig. 8, the majority of the K_{Jc} values from thickness location of 94 mm (disc 1-1.12) are below the MC for 2% fracture probability.

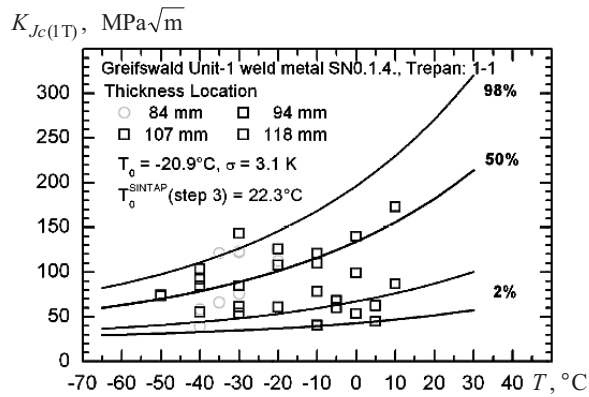


Fig. 8. K_{Jc} values from the thickness locations beyond the welding root versus the test temperature.

The T_0 value of that layer is clearly higher, as compared to the neighboring discs (Fig. 4). Hence, there are brittle zones within the welding seam. Due to the differentiating character of the precracked TS specimen, very small brittle zones can be detected. This implication is confirmed by the metallographic section shown in Fig. 9, where the crack tip is located directly in a fusion zone between two welding beads. One can state that surveillance test series whose specimens originate from different thickness location of the filling layers can lead to a T_0 that represents the brittle constituent. As illustrated in Fig. 8, the 2% MC indexed with T_0^{SINTAP} (step 3) representing the brittle constituent of the dataset envelops the K_{Jc} values except the one that is located directly on the line. As shown in Fig. 4, at the location near the inner RPV wall the evaluated $TT_{41J} = 51^\circ\text{C}$ and thus is close to the reported $T_{K0} = 46^\circ\text{C}$ [2].

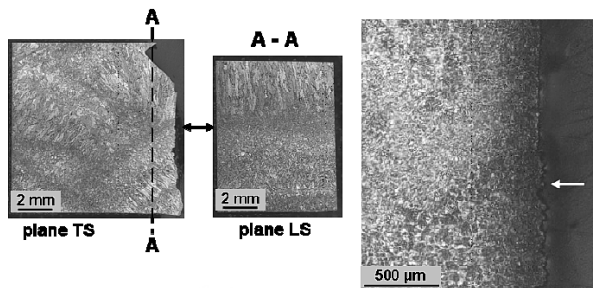


Fig. 9. Metallographic sections of the SE(B) specimen from the thickness location 94 mm.

The level of evaluated upper shelf energy coincides with that expected for WWER-440 weld metals. As mentioned before, $T_K = 30^\circ\text{C}$ was estimated for sub-size impact specimens (type KLST according to DIN EN 10045-1). This T_K is based on a correlation between the $TT_{1,9J}$ transition temperature determined

with KLST specimens and the TT_{41J} transition temperature of standard Charpy-V specimens. The scatter of this correlation of $\pm 35^\circ\text{C}$ is rather high, as well as uncertainty of the applied conversion. Taking into account the difference in the orientation of the specimens and the reirradiation of two cycles, the TT_{41J} estimated with KLST specimens after the recovery-annealing is quite realistic. In this case, the reirradiation causes an increase of TT_{41J} by 21°C . The TT_{41J} transition temperatures of the other thickness locations are lower.

A direct correlation between T_0 and TT_{41J} of the investigated weld metal is questionable due to the different thickness locations (S) of the crack tip and notch root in precracked SE(B) and the reconstituted Charpy-V specimens, respectively. Moreover, the notch root of the reconstituted Charpy-V specimens has a different axial position (T). Hence, the structures at the crack tip and notch root are different. This becomes apparent for the thickness layer of 92 mm (disc 1-1.12) where T_0 agrees with TT_{41J} . Normally, T_0 is expected to be about 40°C lower than TT_{41J} . Based on the results presented here, a low re-embrittlement can be stated for thickness locations close to the inner RPV wall. This is more obvious for the Charpy-V results. The fracture-toughness-based T_0 shows a higher inherent scatter, which is caused by the differentiating character of precracked TS specimens.

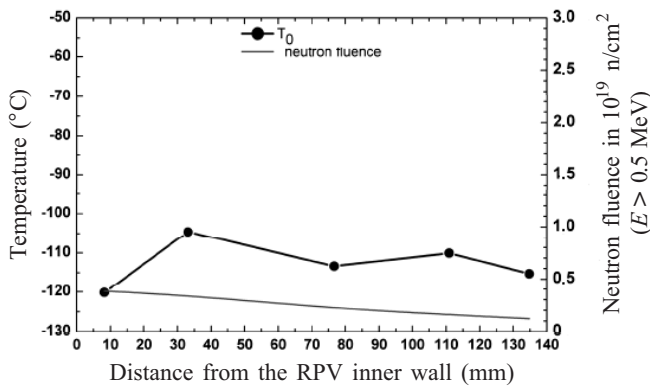


Fig. 10. Course of T_0 and neutron fluence through the RPV wall trepan 1-4 of Greifswald Unit 1.

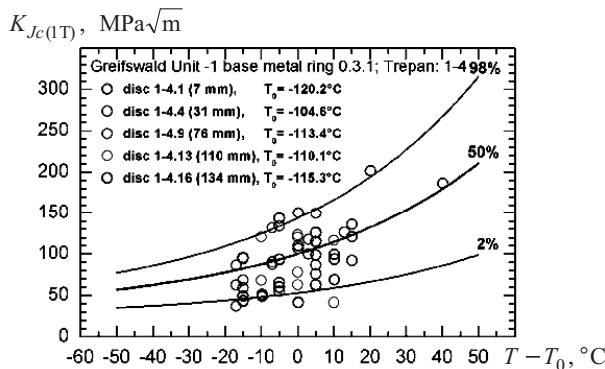


Fig. 11. K_{Jc} values of trepan 1-4 versus the test temperature normalised to T_0 of the individual discs.

Figure 10 depicts the measured reference temperature T_0 from 5 thickness locations, tested and evaluated according to ASTM E1921-05/08, of the base metal

trepan 1-4. The course of the reference temperature T_0 through the RPV wall shows a regular behavior. T_0 varies little over the wall thickness and is under -100°C . The effect of post-annealing reirradiation can be assumed to be low for the base metal of the RPV wall. Figure 11 shows the K_{Jc} values adjusted to the specimen thickness of 1T versus the test temperature normalized to individual T_0 of five thickness locations. The K_{Jc} values generally follow the course of the MC but the scatter here is also large. More than 2% of the values lie outside the fracture toughness range for 2 and 98% fracture probabilities. A possible cause can be the structure of the base metal. Metallographic investigations will be performed to find an explanation for the scatter.

Conclusions. We present first results of the investigations performed with reactor pressure vessel material of the Russian WWER-440 type reactors.

1. Trepanns were taken from the beltline weld and the base metal of the Unit 1 RPV. This RPV was annealed after 15 years of operation and operated for two more years. At first, the trepan of the beltline welding seam was investigated by Master Curve and Charpy V-notch testing. Specimens with TS orientation from 11 locations through the thickness of the welding seam were tested. The differences in T_0 through the beltline welding seam are not the result of the low reirradiation, but are caused by the nonhomogenous structure of the multilayer welding seam. Due to the differentiating character of the precracked TS specimen, very small brittle zones can be detected.

2. With the application of the MC modification in the SINTAP procedure a reference temperature T_0^{SINTAP} can be evaluated which is based on the brittle constituent of a dataset. There are remarkable differences between T_0 and T_0^{SINTAP} indicating macroscopic inhomogeneous weld metal for some thickness locations. Specimens with LS orientation from 5 locations through the thickness of the RPV from the base metal trepan 1-4 were tested and evaluated with the Master Curve. The course of the reference temperature T_0 in the base metal shows a regular behavior over the RPV wall thickness. T_0 varies little over the wall thickness and is under -100°C . There is remarkable scatter in the K_{Jc} values and more K_{Jc} values than expected lie below the 2% fractile which indicates macroscopic inhomogeneity.

3. The effect of post-annealing reirradiation in the base metal of the RPV wall can be assumed to be low for the investigated base metal, as well as for the weld metal. The orientations for base and weld metal show that the crack front is located in a uniform structure, but nevertheless the scatter of the K_{Jc} values is high.

4. The crack tip position in the multilayer welding seam is crucial. A comparison regarding the orientation of SE(B) specimens with the Master Curve will follow. Generally, the effect of the recovery annealing was confirmed with the fracture toughness and Charpy-V testing. The TT_{41J} estimated with subsized KLST impact specimens after the annealing was confirmed by the testing of standard Charpy V-notch specimens.

Acknowledgment. This study was funded by the German Federal Ministry of Economics and Technology (Reactor Safety Research Project Grant No. 1501331).

Резюме

Представлено результати дослідження матеріалів бандажного зварного шва та кільця основного металу посудини тиску першого блоку реактора типу ВВЕР-440/230. Досліджували круглі вирізки матеріалу (тріпани) після радіаційного опромінення з наступним відпалом і повторним опроміненням. Основна задача робочої програми досліджень – отримання розподілу механічних характеристик реакторних сталей по товщині стінки реактора. Згідно зі стандартом ASTM E192 визначали базисну температуру T_0 з метою оцінки розподілу в'язкості руйнування по товщині стінки реактора.

1. J. Konheiser, U. Rindelhardt, H.-W. Viehrig, et al., "Pressure vessel investigations of the former Greifswald NPP: Fluence calculations and Nb based fluence measurements," in: Proc. ICONE14/FEDSM2006, Contribution ICONE 14-89578 (2006).
2. R. Ahlstrand, E. N. Klausnitzer, D. Langer, et al., "Evaluation of the recovery annealing of the reactor pressure vessel of NPP Nord (Greifswald) Units 1 and 2 by means of subsize impact specimens," in: E. Lendell (Ed.), *Radiation Embrittlement of Nuclear Reactor Pressure Vessel Steels: An International Review* (Fourth Volume), ASTM STP 1170, Philadelphia (1993), pp. 321–343.
3. H.-W. Viehrig, U. Rindelhardt, and J. Schuhknecht, "Post mortem investigations of the NPP Greifswald WVER-440 reactor pressure vessels," in: Proc. of 19th Int. Conf. on *Structural Mechanics in Reactor Technology* (SMiRT19, 12–17 August, Toronto) (2007).
4. L. M. Davies, *A Comparison of Western and Eastern Nuclear Reactor Pressure Vessel Steels*, AMES Report No. 10, EUR 17327, European Commission, Luxembourg (1997).
5. M. Brumovsky, M. Valo, A. Kryukov, et al., *Guidelines for Prediction of Irradiation Embrittlement of Operating WVER-440 Reactor Pressure Vessels*, IAEA-TECDOC-1442, IAEA, Vienna (2005).
6. *ASTM E399. Standard Test Method for Plane-Strain Fracture Toughness of Metallic Materials*, Annual Book of ASTM Standards, West Conshohocken, PA (2006).
7. *ASTM E1921-05. Standard Test Method for Determination of Reference Temperature, T_0 , for Ferritic Steels in the Transition Range*, Annual Book of ASTM Standards, PA (2006).
8. *Structural Integrity Assessment Procedures for European Industry (SINTAP)*, Final Version: WEM/SINTAP/PROC_7/CONTENTS REGP (05.11.99), November, 1999.
9. *PNAÉ-G-7-002-086. Regulatory Guide for Strength Calculation of Nuclear Power Plant Equipments and Piping* [in Russian], Atoménergoizdat, Moscow (1989).

Received 21. 06. 2009